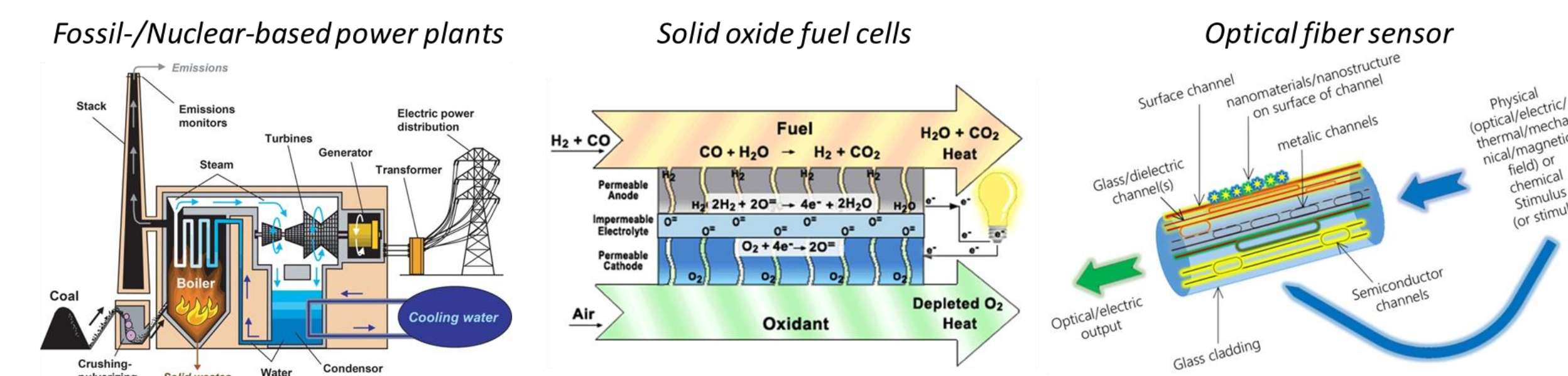


## Introduction

- For advanced real-time monitoring and control of gas species in combustion environments, development of efficient sensing platforms and new sensor materials able to work under harsh environments are required.
- Semiconducting optical-based sensor platforms show promise. MO<sub>x</sub> metal-oxides and ABO<sub>3</sub> perovskite-oxides can be attractive for high-temperature applications due to their high decomposition temperatures and structural stability; ABO<sub>3</sub> allows tunable electronic and optical properties owing to flexible choices of A, B dopants and forming oxygen non-stoichiometric point-defects



- Combining first-principles modeling with machine learning is a powerful tool to screen and design functional materials for sensing application under harsh environments. It can be also used to determine the sensing mechanisms and the performance of the high-temperature sensors.

## Methods

- Density functional theory (DFT):** PAW-PBE(+U) XC in GGA
  - Energies of formation of point defects (La and Mg dopants, O vacancies)

$$\Delta H(\text{SrTiO}_3, \text{def}) = E(\text{SrTiO}_3, \text{def}) - E(\text{SrTiO}_3) - \sum_i n_i \mu_i$$

- Optical properties calculated from frequency-dependent dielectric function

$$\epsilon(\omega) = \epsilon_1(\omega) + i\epsilon_2(\omega) = (n + ik)^2 = \frac{4\pi i}{\omega} \sigma(\omega)$$

- Allen-Heine-Cardona (AHC) theory**
  - Lattice thermal expansion and, most dominantly, electron-phonon coupling contribute to renormalization of the band gaps
  - Prediction of electron-phonon coupling effect on eigenstate energy level shifts  $\Delta\epsilon_{nk}(T)$ , in harmonic phonon approximation

$$\Delta\epsilon_{nk}(T) = \frac{1}{N_q} \sum_{q,v} a_{q,v}^{(2)} \frac{1}{\omega_{q,v}} \left[ \frac{1}{2} + n_B(\omega_{q,v}, T) \right]$$

- Fit to empirical O'Donnell model

$$E_g = E_0 - S \langle \hbar\omega \rangle \left[ \coth\left(\frac{\langle \hbar\omega \rangle}{2k_B T}\right) - 1 \right]$$

- P. B. Allen, V. Heine, *J. Phys. C* **9**(1976)2305-12;
- P. B. Allen, M. Cardona, *Phys. Rev. B* **23**(1981)1495-1505

- K.P. O'Donnell, X. Chen, *Appl. Phys. Lett.* **58**(1991)2924-26.

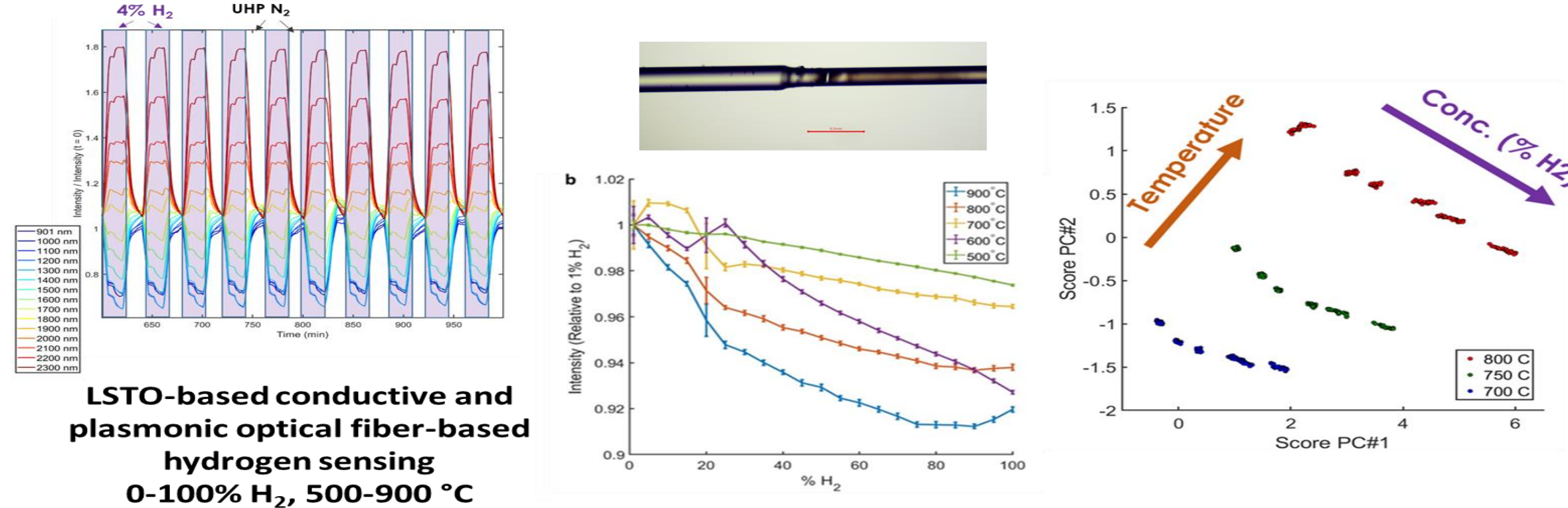
- Machine Learning**
  - Principal component analysis applied to combine 37 features into one reduced feature for each parameter in the O'Donnell model

$E_0$	$S$	$\langle \hbar\omega \rangle$
<b>Formation energy</b> , molar density, melting point	<b>Atomic mass, Electron-Phonon Debye temperature</b> , thermal conductivity, heat of vaporization, speed of sound, boiling point, melting point	<b>Entropy of formation</b> , heat capacity, volume, density

- Bolded features were found to have the highest absolute value of the eigenvector (high relative importance in their respective principal component)
- Gaussian process (GP) regression models were trained separately for each of the three parameters

## Doped Perovskite Sensing Layers on Optical Fiber

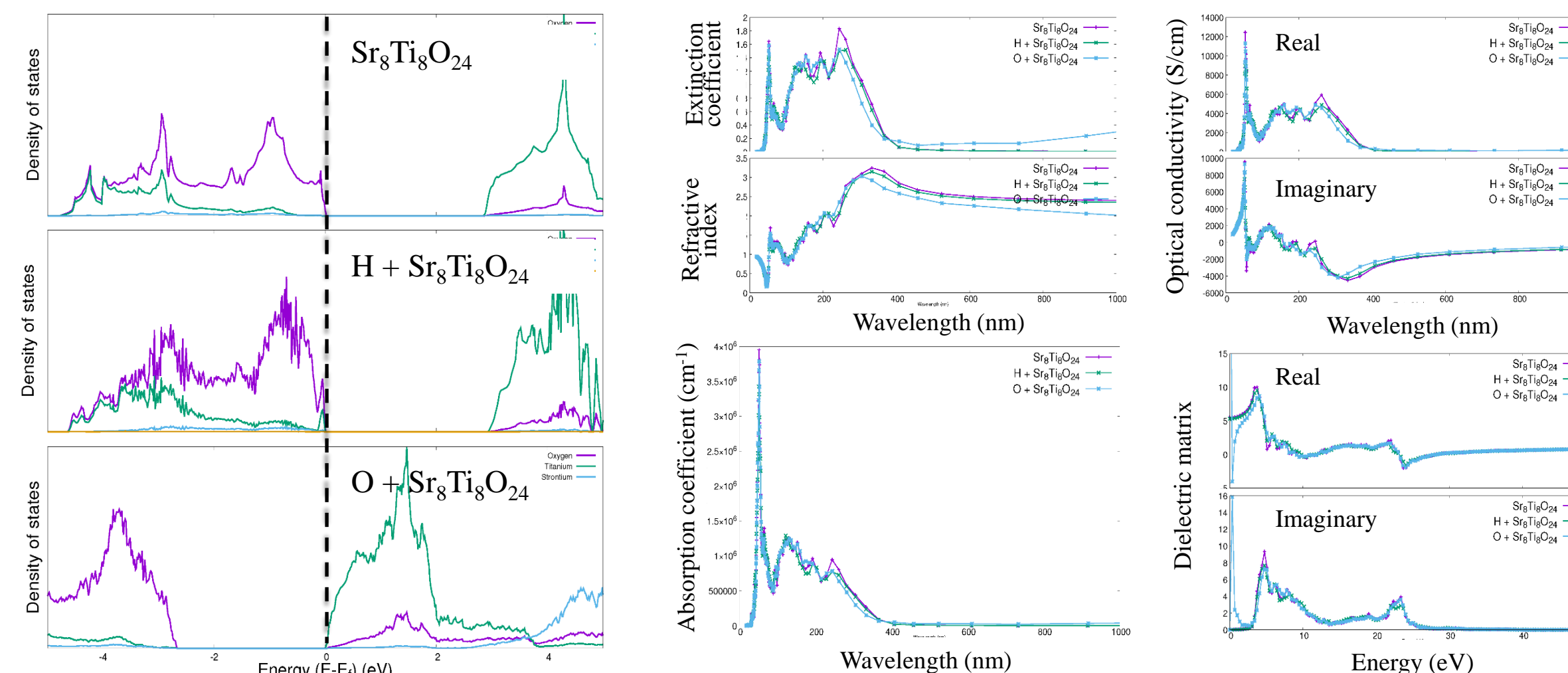
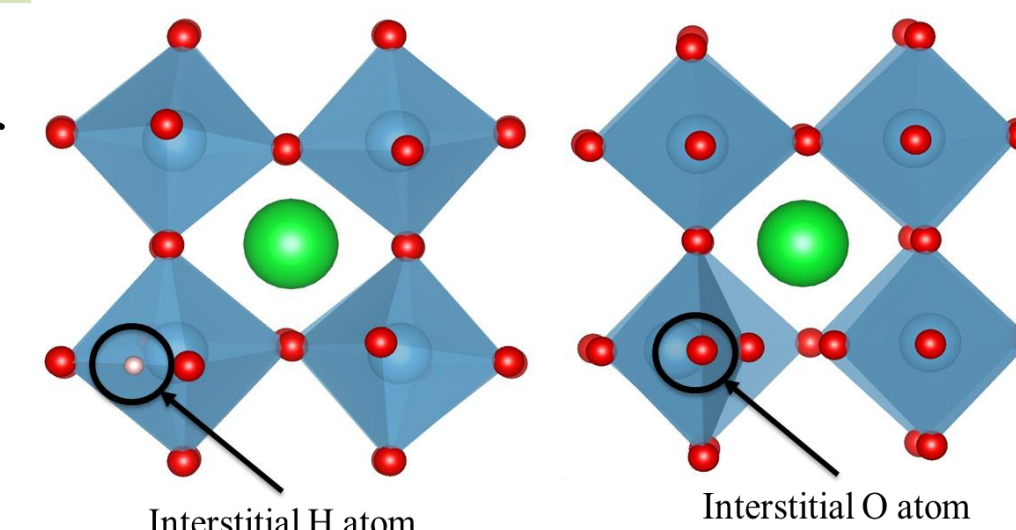
- As a functional sensing layer on evanescent-field based optical fiber sensors, A- or B-site doped can operate as a versatile, high-T sensor for reducing or oxidizing gas streams.
- La-doped SrTiO<sub>3</sub> acts like an *n*-type doped semiconductor under reducing conditions – demonstrating **an effective high-T sensing material for H<sub>2</sub>**.



- Other SrTiO<sub>3</sub>-based systems such as SrFe<sub>x</sub>Ti<sub>1-x</sub>O<sub>3</sub> (SFTO) and Mg-doped SrTiO<sub>3</sub> can act as *p*-type doped semiconductors under oxidizing conditions and show promise for **high-T stable oxygen sensing**.

## Interstitial Hydrogen and Oxygen Impurities

- Interstitial H atom preferably binds to O atom in STO leading to breaking of octahedral symmetry
- Interstitial O atom bonds to apical O causing distortion of Ti octahedral but does not break symmetry of the crystal
- Incorporation of H, O interstitials alters SrTiO<sub>3</sub> electronic, optical properties as both can act as electron donors to system
- H introduces defect states at VBM above Fermi level without significant changes to bandgap, optical absorption, or the dielectric matrix
- O induces *n*-type conductivity, evident in DOS and Drude peak in imaginary component of dielectric matrix; causes peak shift in optical conductivity to lower wavelength (higher photon energy)

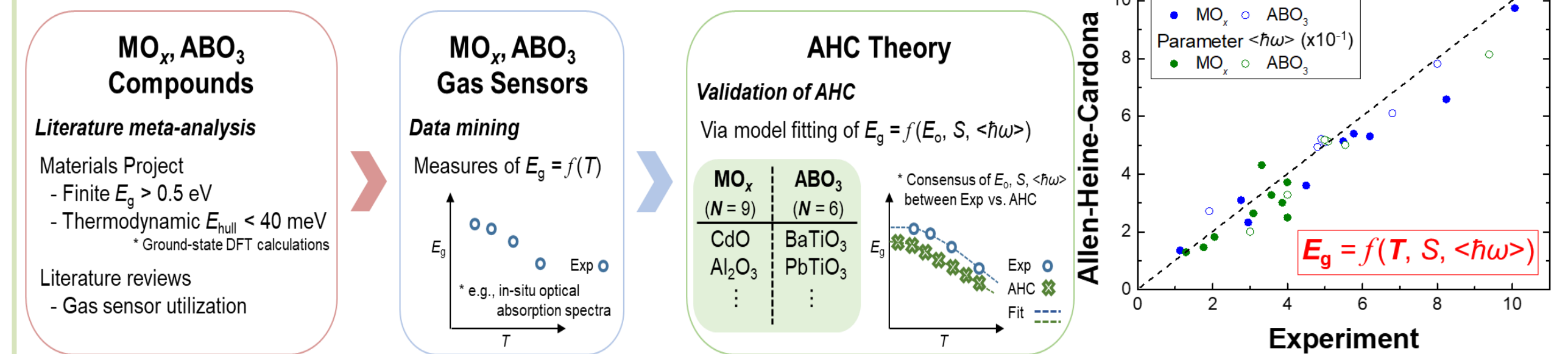


## Publications

- J. Park *et al.*, *Phys. Chem. Chem. Phys.* **22**(2020) 27163-72; *ACS Appl. Mater. Interfaces* **13**(2021) 17717-25; *J. Phys. Chem. C* **125**(2021) 22231-38; **126**(2022)8832-38; *Chem. Mater.* **34**(2022)6108-15
- Y.-N. Wu *et al.*, *J. Phys. Chem. C* **122**(2018) 22642-49; *J. Phys. Chem. Lett.* **11**(2020) 2518-23; *J. Phys. Condens. Matter* **32**(2020) 405705.
- T. Jia *et al.*, *RSC Adv.* **7**(2017) 38798-804; *Phys. Chem. Chem. Phys.* **22**(2020) 16721-26; *Applied Energy* **281**(2021)116040; *J. Phys. Chem. C* **125**(2021) 12374-81; **126**(2022)11421-25
- Y. Duan *et al.*, *J. Solid State Chem.* **256**(2017) 239-251.
- S. Nations, *et al.*, *RSC Adv.* **11**(2021) 22264-72; *Mater. Adv.* **3**(2022)3897-3905; *Nanomaterials* **13**(2023)276
- T. Nandi, L. Chong, J. Park, W. A. Saidi, B. Chorpeneing, S. Bayham, Y. Duan, *AIP Advances* **14**(3)(2024)035231.

## Applicability of AHC Theory via Machine Learning

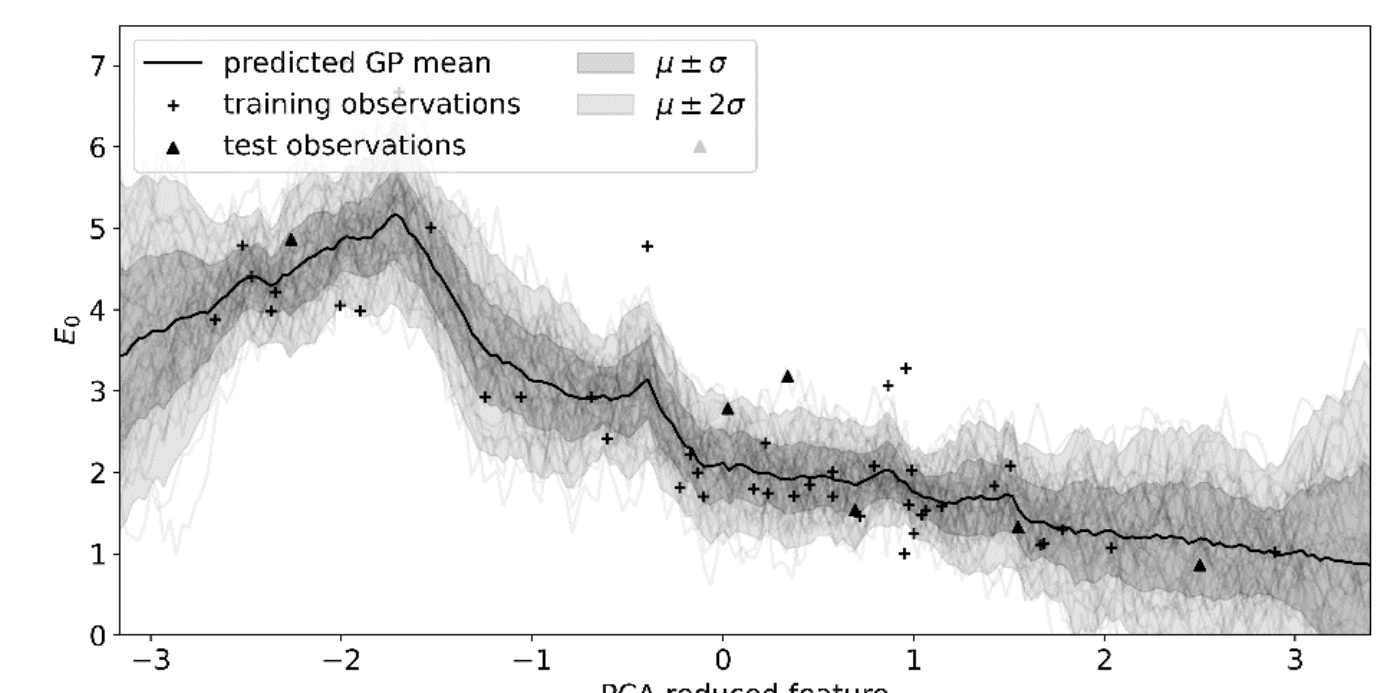
- Assess the consensus between the AHC theory and the measurements on temperature dependence of the band gaps in MO<sub>x</sub> and ABO<sub>3</sub>
  - In conjunction with O'Donnell model to quantify the temperature dependence of band gaps using well-defined parameters



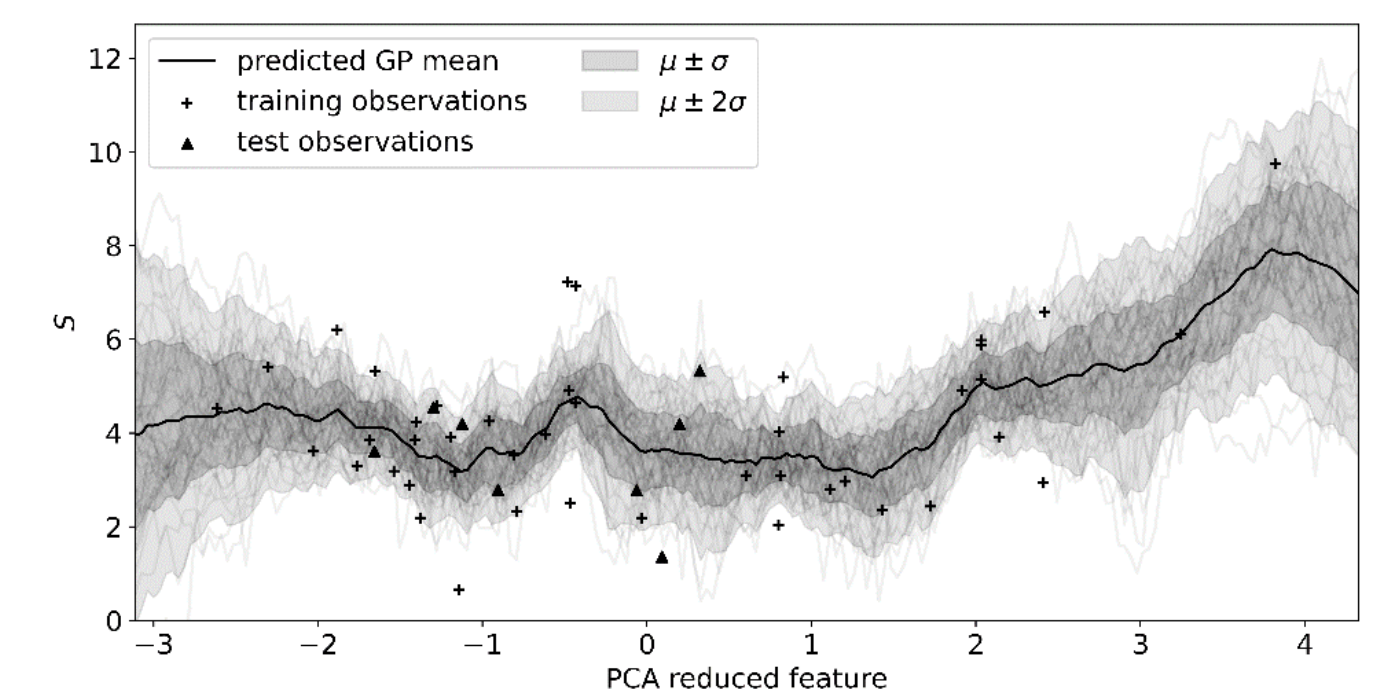
- Machine learning (ML) for predicting O'Donnell model parameters in MO<sub>x</sub>
  - Ultimately enables ML prediction of the temperature dependence of band gaps

## Machine Learning

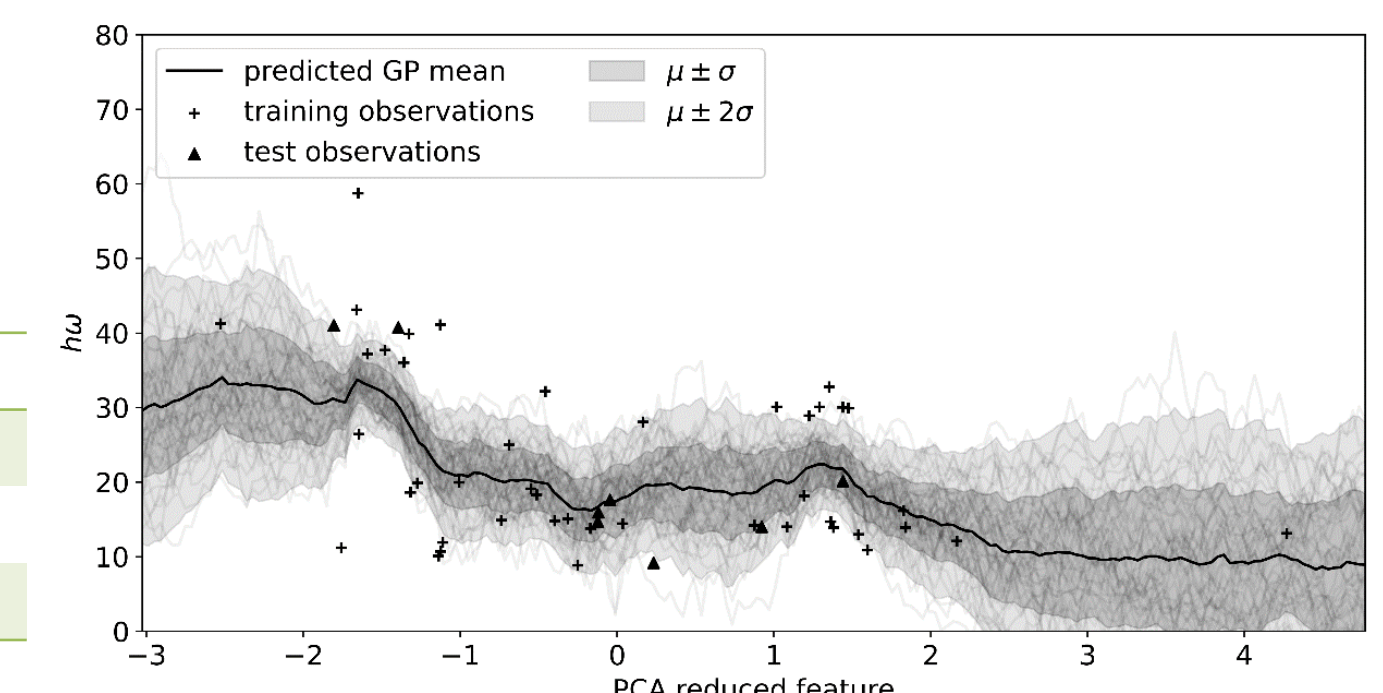
- O'Donnell parameters have been calculated by DFT for 54 metal oxides and are accepted as ground truth for the development of the ML models



- Most of the training data as well as the test predictions fall within the predicted mean μ ± 2σ region



- Region of uncertainty is observed to be larger where the training points are sparsely populated and increases significantly for regions outside of the training dataset



	RMSE	MAE
$E_0$ (eV)	0.8863	0.6729
$S$	1.142	0.8881
$\hbar\omega$ (meV)	6.943	5.414

- SnO<sub>2</sub> used as an example test data point for the combined prediction of parameters to calculate band gap

SnO <sub>2</sub>	Predicted	Observation
$E_0$ (eV)	2.8101 ± 0.8618	1.9978
$S$	3.8541 ± 2.1652	2.35
$\hbar\omega$ (meV)	30.2017 ± 6.3966	40.77
$E_g$ (eV) @ 1000 K	2.2555	1.681